JREE: Vol. 6, No. 2, (Spring 2019) 22-29

Journal of Renewable Energy and Environment

Research Article

Journal Homepage: www.jree.ir

Optimization and Experimental Approaches to the Direct Methanol Fuel Cell Stack Using a Response Surface Methodology

Shima Sharifi[a], Rahbar Rahimi[a*], Davod Mohebbi-Kalhori[a], Can Ozgur Colpan[b]

[a] *Department of Chemical Engineering, Faculty of Engineering and Center for Renewable Energy Research, University of Sistan and Baluchestan, Zahedan, Iran.*
[b] *Department of Mechanical Engineering, Dokuz Eylul University, Tinaztepe Yerleskesi, Buca, Izmir, 35397, Turkey.*

PAPER INFO

Paper history:
Received 05 August 2019
Accepted in revised form 21 October 2019

Keywords:
Direct Methanol Fuel Cell Stack
Maximum Power Density
Regression Model
Response Surface Methodology

ABSTRACT

The power density of a direct methanol fuel cell (DMFC) stack as a function of temperature, methanol concentration, oxygen flow rate, and methanol flow rate was studied using a response surface methodology (RSM) to maximize the power density. The operating variables investigated experimentally include temperature (50-75 °C), methanol concentration (0.5-2 M), methanol flow rate (15-30 ml min^{-1}), and oxygen flow rate (900-1800 ml min^{-1}). A new design of the central composite design (CCD) for a wide range of operating variables that optimize the power density was obtained using a quadratic model. The optimum conditions that yield the highest maximum power density of 86.45 mW cm^{-2} were provided using 3-cell stack at a fuel cell temperature of 75 °C with a methanol flow rate of 30 ml min^{-1}, a methanol concentration of 0.5 M, and an oxygen flow rate of 1800 ml min^{-1}. Results showed that the power density of DMFC increased with an increase in the temperature and methanol flow rate. The experimental data were in good agreement with the model predictions, demonstrating that the regression model was useful in optimizing maximum power density from the independent operating variables of the fuel cell stack.

1. INTRODUCTION

Over the past decade, the demand for renewable and clean energy resources, such as wind, solar, geothermal, biomass, hydropower, and fuel cells, have increased significantly. In particular, due to a high energy density, the low-cost and easy storage and handling of methanol, and low operating temperatures, direct methanol fuel cells (DMFCs) are promising candidates to produce electricity for portable electronic applications like laptops and mobile phones [1,2]. The main challenges associated with this type of fuel cells are low power density due to slow reaction kinetic at the anode and cathode chambers, methanol crossover, low stability and durability, and water management.

Many factors affect the DMFC performance such as concentration of methanol, fuel and air flow rates, and operating temperature. Several researchers have investigated the effects of these operating conditions on the performance of DMFC. For example, Ge and Liu [3] experimentally studied the effects of the cell temperature, cathode humidification temperature, methanol concentration, anode and cathode flow rates on the DMFC performance. They reported that only the temperature of cathode humidification did not affect cell performance. Argyropoulos et al. [4] showed that the methanol concentration, cathode air pressure, and methanol flow rate could significantly affect the DMFC voltage dynamic response. Seo and Lee [5] examined oxygen or air as an oxidant to study the effects of cell temperature, flow rate, methanol concentration, humidification temperature, and backpressure at the cathode on DMFC performance. The results showed that oxygen exhibited greater instrumentality in the higher DMFC performance than the air. Jung et al. [6] investigated the effects of Nafion types, cell temperature, and concentration of methanol on the single cell, and showed that the performance of the DMFC enhanced with an increase in the cell temperature. According to their results, maximum current density was obtained using Nafion 112 at a fixed voltage of 0.55 V when 2.5 M methanol was used.

In order to obtain the effect of different parameters on the performance of a fuel cell system extensively, a large number of experiments are needed. The governing equations of change and rates as applicable to DMFC for having an insight into the experimental approach are summarized in Table 1 [7].

The common approaches of experiments were implemented by changing only one variable at a time, while maintaining the other variables constant. This approach does not take into account the effects of a possible interaction between the input variables. The design of experiment (DOE) and statistical tools reduce the number of experiments and experimental time and cost. In addition, the DOE method can be used to determine the impacts of the operating variables and their interactions on fuel cell performance and find the operating and design conditions that yield the optimum performance. One-factor design, factorial designs, two-level fractional factorial, response surface methodology (RSM), and Taguchi orthogonal arrays are some of the most common DOE types. Among the DOE methods, RSM is a strong tool for optimization, which is based on a fit between one polynomial equation and the data of the experiments. In this method, linear or square polynomials equations are applied to describe the behavior of the system by considering the effect of independent variables and their interaction effects and, consequently, to explore the experimental conditions that optimize the system studied [8]. Selecting the most important independent variables, choosing the experimental design, performing the experimental test, fitting a polynomial

*Corresponding Author's Email: rahimi@hamoon.usb.ac.ir (R. Rahimi)

equation, evaluating the fitted model, and obtaining the optimal values are the steps in applying the RSM method. This method has been applied in fuel cells in some studies found in the literature [9-13].

For example, Taymaz et al. [9] optimized the DMFC operating conditions by using a quadratic model for the RSM. They investigated the effects of methanol and oxygen flow rates, the temperature of cell, and humidification temperature on the performance. Silva et al. [10] studied the effects of parameters such as temperature, air and methanol flow rates, concentration methanol, and air relative humidity on the DMFC power density using RSM. The results indicated that the effective operating variables on the power density included temperature, air flow rate, and methanol concentration. Charoen et al. [11] employed RSM to investigate the effects of flow rate and concentration of alcohol and operating temperature on the DMFC and direct ethanol fuel cell (DEFC) performance. They found that alcohol concentration and operating temperature had significant influence on the power density. Yuan et al. [12] found that the performance was significantly affected by the flow rate and concentration of methanol and cell temperature through RSM in the air-breathing micro direct methanol fuel cell (μDMFC). Ordonez et al. [13] obtained a model for the fuel cell system using the DOE methodology. In order to build up a model for DMFC, Central Composite Design (CCD) and the Steepest Ascent Method (SAM) were used to yield the maximum power density amounts.

Many single cells are connected in series to form fuel cell stack in order to increase the power output and achieve high volumetric power density for practical applications. There are many mathematical modeling and empirical studies on the polymer electrolyte membrane (PEM) fuel cell stacks that predict fuel cell performance and investigate the operating and design conditions effects on the fuel cell (e.g., [14–25]). However, fewer papers exist on the performance improvement of DMFC stacks through numerical and experimental studies in the literature. For example, Argyropoulos et al. [26] presented a model for DMFC stack that predicts the pressure drop of an individual fuel cell and the flow distribution through stack internal manifolds. Furthermore, Argyropoulos et al. [27–29] developed models that describe the stack voltage, fluid distribution from the stack manifolds, pressure, and thermal management of the stack. Kim et al. [30] investigated the performance of the DMFC stack under operating conditions such as the reactant flow rate, concentration of methanol, and the reactant direction in the stack. Lohoff et al. [31] used the RSM to describe the water permeation, cell voltage, and methanol crossover of a DMFC short stack. The results indicated that the behavior of the stack was affected by input variables including temperature, methanol concentration, and current density. Santiago et al. [32] developed a computer-aided automated system to quickly design DMFC stacks, where mass, volume, and fuel consumption are optimized.

In all of the above literature pieces, the optimization of operating conditions of a single cell was investigated using the RSM; however, in this work, a 3-cell stack with two parallel-serpentine flow channels was considered to be used in portable applications. In this study, response surface methodology (RSM) with a Central Composite Design (CCD) was applied using Design-Expert 10.0.7 to optimize the operating parameters and investigate the effect of cell temperature, methanol and oxygen flow rates, and methanol concentration on the power density of a DMFC stack.

Table 1. The equations of change and rates for anode and cathode [7].

DMFC relations	Equations No.
$\rho\nabla.u = Q_{br}$	(1)
$\frac{\rho}{\varepsilon_p}\left((u.\nabla)\frac{u}{\varepsilon_p}\right) = \nabla.\left[-p + \frac{\mu}{\varepsilon_p}(\nabla u + (\nabla u)^T) - \frac{2}{3}\frac{\mu}{\varepsilon_p}(\nabla.u)\right] - \left(\frac{\mu}{\kappa} + \frac{Q_{br}}{\varepsilon_p^2}\right)u$	(2)
$\nabla.(-D_{i,eff}\nabla c_i) + u.\nabla c_i = R_i$	(3)
$i_l = -\sigma_l\nabla\phi_l$, $\nabla.i_l = Q_l$	(4)
$i_s = -\sigma_s\nabla\phi_s$, $\nabla.i_s = Q_s$	(5)
In Eq. (1), Q_{br} is the mass source term, which is zero in the flow channels and the diffusion layers, while its value in the catalyst layers can be calculated through Eq. (6).	
$Q_{br} = \sum_m\sum_i R_{i,m}M_i$	(6)
The effective diffusivity, $D_{i,eff}$, is defined by the Bruggeman equation in porous media: $D_{i,eff} = \varepsilon^{1.5}D_i$	(7)
$j_a = \frac{ai_{oa}^{ref}C_{MeOH}\exp((\alpha_a F/RT)\eta_a)}{C_{MeOH} + K_c\exp((\alpha_a F/RT)\eta_a)}$ Reaction rate of methanol (anode)	(8)
$j_c + j_{xover} = ai_{oc}^{ref}\frac{C_{O_2}}{C_{O_2}^{ref}}\exp\left(\frac{-\alpha_c F}{RT}\eta_c\right)$ Reaction rate of oxygen (cathode)	(9)
$j_{xover} = \frac{6FN_{MeOH}^{*M\|CCL}}{t_{ccl}}$	(10)
$\eta_a = \phi_s - \phi_l - E_a^{Eq}$	(11)
$\eta_c = \phi_s - \phi_l - E_c^{Eq}$	(12)

2. EXPERIMENTAL

2.1. DMFC performance tests

Commercially available membrane electrode assembly (MEA) with 25 cm^2 active area was used in a 3-cell DMFC stack system (Yangtze Energy Technologies, Inc.). Each MEA is composed of anode and cathode catalyst layers having 4 mg_{metal} cm^{-2} Pt-Ru/C and 4 mg_{metal} cm^{-2} Pt/C catalyst loadings, respectively, two gas diffusion layers (or backing layers), and a Nafion® 117 membrane. Two parallel-serpentine channels with a depth of 1 mm, 1.2 mm width, and 0.7 mm rib were machined on the bipolar plates, which are made of composite graphite. A schematic of the bipolar plate is presented in Figure 1. Two copper current collector plates, which are coated with gold, and two aluminum end plates were used. Two gaskets (0.1 mm) were employed in order to seal the stack on the anode and cathode sides of each cell. The MEA was placed between the gaskets, and 5 Nm torque was applied for tightening the fuel cell stack. After assembling the fuel cell stack, the leakage test was performed. The stack was controlled by a DMFC test station (Asian Hydrogen New Science Co.), as shown in Figure 2. A peristaltic pump was used to inject methanol solution on the anode side. The flow rate of oxygen was controlled by the mass flow controller on the cathode side. The temperature controller measures the fuel cell stack and cathode humidifier temperatures. During the experiments, the pressure at the inlets of the test station was kept at 2-3 bar. The current density-voltage and current density-power density curves of the stack were recorded using a computer-aided DMFC test station. For each voltage point along the polarization curve, the waiting time of 10 s was applied to obtain a steady value. The stack specification is listed in Table 2.

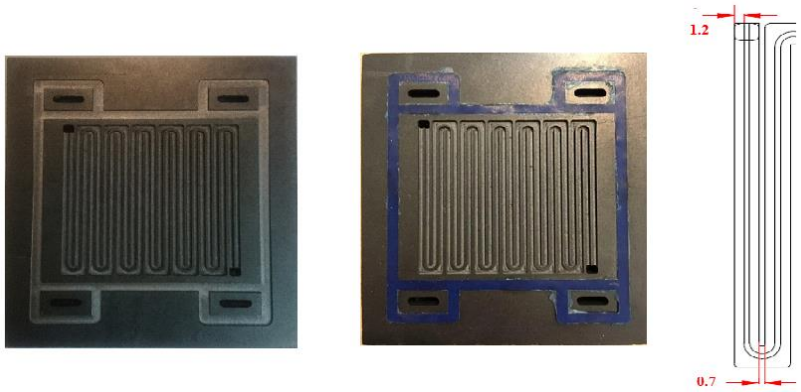

Figure 1. Schematic of the parallel-serpentine flow fields. Graphite with the silicon gasket (center).

Figure 2. Photograph of the DMFC stack test station.

Table 2. DMFC stack specification.

Components	Specifications
MEA	
Membrane	PFSA (Nafion 117)
Thickness of membrane	175 µm
Active area	25 cm^2
Catalyst loading of anode	Pt-Ru/C, 4 mg_{metal}/cm^2
Catalyst loading of cathode	Pt/C, 4 mg_{metal}/cm^2
Stack	
Cells number	3
Current collector	Gold-coated copper
Bipolar plate	Composite graphite with two parallel-serpentine flow fields

2.2. Design of experiments: The selection of optimum operating conditions

The CCD is one of the most important design methods for fitting second-order response surface models. The design involves 2k axial or star points, 2^k factorial points, and n_c center runs (where k is the number of variables). The interaction and quadratic terms of the equation were estimated using factorial and axial points, respectively. The center runs were also used to estimate pure error and contributed to the estimation of quadratic terms [8].

In the present study, response surface methodology was used to optimize the operating variables of a DMFC stack by employing a central composite design for four independent variables at three levels. These operating variables are cell temperature, methanol flow rate, methanol concentration, and

oxygen flow rate. Accordingly, the number of experiments was 28 ($=2^k+2k+n_c$), where n_c is the number of replications at the center point (=4). The levels of the operating parameters are shown in Table 3, while the experimental results of the maximum power density for CCD are given in Table 4.

The quadratic polynomial equation model was used to determine the correlation between the independent and dependent (response) variables according to the following equation [8]:

$$Y = \beta_0 + \sum_{i=1}^{k}\beta_i x_i + \sum_{i=1}^{k}\beta_{ii} x_i^2 + \sum_{i=1}^{k}\sum_{j=i+1}^{k}\beta_{ij} x_i x_j + \varepsilon \quad (13)$$

where Y is the response (power density), X_i and X_j are the independent variables, β_0 is the constant coefficient, β_i, β_{ii}, and β_{ij} are the linear, quadratic, and second-order interaction coefficients, and ε is the random error.

Table 3. Independent variables and their levels employed for the experimental design.

Operating variables	Levels		
	-1	0	1
Temperature (°C)	50	62.5	75
Methanol concentration (mol lit^{-1})	0.5	1.25	2
Methanol flow rate (ml min^{-1})	15	22.5	30
Oxygen flow rate (ml $^{-1}$min)	900	1350	1800

Table 4. Results of central composite design and experimental conditions.

Run	Temperature (°C)	Methanol concentration (M)	Methanol flow rate (ml/min)	Oxygen flow rate (ml/min)	Maximum power density (mW/cm^2)
1	62.5	0.5	22.5	1350	75.56
2	62.5	1.25	22.5	900	66.17
3	75	2	30	900	70.52
4	50	0.5	15	1800	67.25
5	50	2	30	900	64.37
6	75	0.5	15	900	82.35
7	50	0.5	30	1800	68.21
8	75	2	30	1800	80.51
9	62.5	2	22.5	1350	72.65
10	62.5	1.25	22.5	1350	70.86
11	50	0.5	15	900	64.27
12	50	2	15	900	64.02
13	62.5	1.25	22.5	1350	70.01
14	50	2	15	1800	64.15
15	75	1.25	22.5	1350	78.49
16	75	2	15	900	66.82
17	75	2	15	1800	72.42
18	62.5	1.25	15	1350	73.41
19	62.5	1.25	22.5	1800	71.15
20	75	0.5	30	1800	86.45
21	50	1.25	22.5	1350	70.37
22	62.5	1.25	22.5	1350	70.42
23	62.5	1.25	30	1350	74.64
24	50	0.5	30	900	67.21
25	50	2	30	1800	65.52
26	75	0.5	15	1800	83.79
27	62.5	1.25	22.5	1350	68.32
28	75	0.5	30	900	83.55

3. RESULTS AND DISCUSSION

The results of the analysis of variance (ANOVA) for the quadratic model are given in Table 5. As Table 4 shows, the quadratic polynomial model was highly significant (F-value = 15.11). The probability values less than 0.05 (p-value < 0.0001) indicate that model terms are significant. The value of regression coefficient (R^2 = 0.9421) shows that the quadratic model is suitable to describe the relationship between experimental results and parameters.

The following regression equation in terms of coded factors for maximum power density can be expressed as follows:

$$\text{Maximum power density} = +71.56 +6.09A -3.20B +1.25C +1.68D -2.31AB +0.63AC +0.92AD +0.36BC +0.53BD +0.30CD +1.76A^2 +1.44B^2 +1.35C^2 -4.01D^2 \quad (14)$$

diagnostic plots are used to check the model adequacy. In Figure 3, the normal probability plot of the studentized residuals was developed for the maximum power density. The normality assumption is satisfied since the points of this plot lie reasonably close to a straight line. Figure 4 presents the residuals plot versus the predicted response. Based on the random scattering of the residual shown in Figure 4, the variance of the observation is constant for all values of response. The correlation between the actual and predicted values of power density for checking model adequacy is given in Figure 5. It is clear that the actual values are scattered close to the straight line.

Table 5. ANOVA for the fitted quadratic polynomial model of power density.

Source	Sum of squares	df	Mean square	F-value	P-value Prob>F
Model	1091.19	14	77.94	15.11	< 0.0001
A-temperature	666.58	1	666.58	129.21	< 0.0001
B-methanol concentration	184.86	1	184.86	35.83	< 0.0001
C-methanol flow rate	28.12	1	28.12	5.45	0.0363
D-oxygen flow rate	50.60	1	50.60	9.81	0.0079
AB	85.58	1	85.58	16.59	0.0013
AC	6.31	1	6.31	1.22	0.2888
AD	13.51	1	13.51	2.62	0.1296
BC	2.06	1	2.06	0.40	0.5384
BD	4.56	1	4.56	0.88	0.3644
CD	1.48	1	1.48	0.29	0.6007
A^2	8.03	1	8.03	1.56	0.2343
B^2	5.32	1	5.32	1.03	0.3284
C^2	4.73	1	4.73	0.92	0.3560
D^2	41.57	1	41.57	8.06	0.0140
Residual	67.07	13	5.16		
Lack of fit	63.35	10	6.33	5.11	0.1030
Pure error	3.72	3	1.24		
Cor total	1158.26	27			
R-squared	0.9421				
Adj R-squared	0.8797				

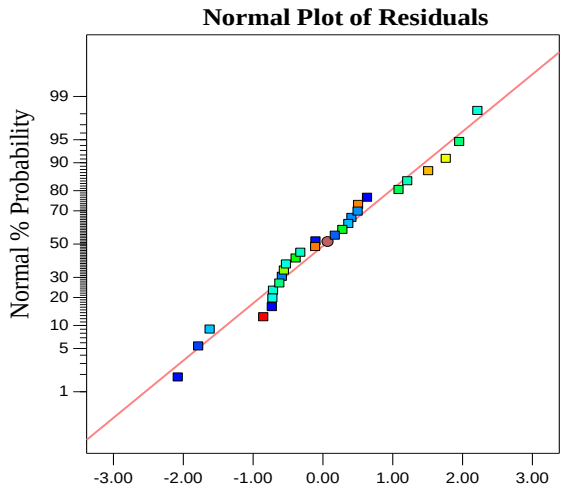

Figure 3. Normal probability plot of the standardized residuals.

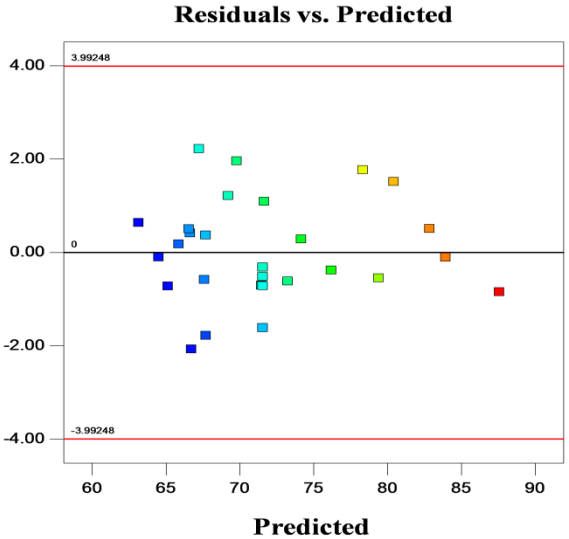

Figure 4. Plot of residuals versus the predicted response.

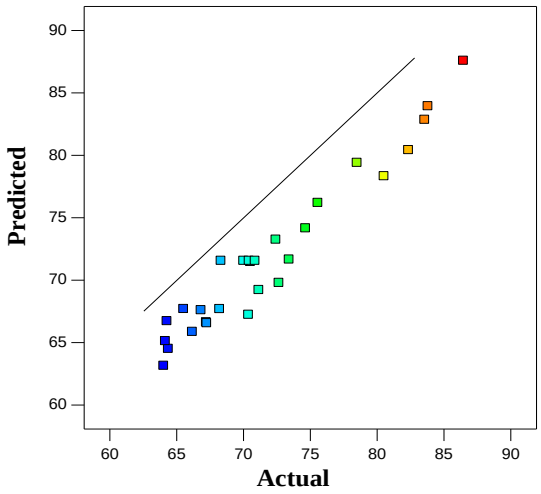

Figure 5. Actual versus predicted values for maximum power density.

The effects of methanol concentration and cell temperature on the response (power density) are presented in Figure 6 when the methanol and oxygen flow rates are a constant of 30 ml min^{-1} and 1800 ml min^{-1}, respectively. It can be seen that, at a constant concentration of methanol, power density increased with the increase of temperature from 50 to 75 °C. This is because both reaction kinetics improve with temperature at the anode and cathode and activation loss decreases according to the Arrhenius equation. The maximum power density was achieved at the temperature and methanol concentration of 75 °C and 0.5 ml min^{-1}, respectively. In Figure 7, the 3D response surface and contour plots are developed for the power density with changing the methanol flow rate and methanol concentration. Power density decreases as the methanol concentration increases due to the methanol crossover. The maximum power density was predicted at a high level of the methanol flow rate and a low level of the methanol concentration.

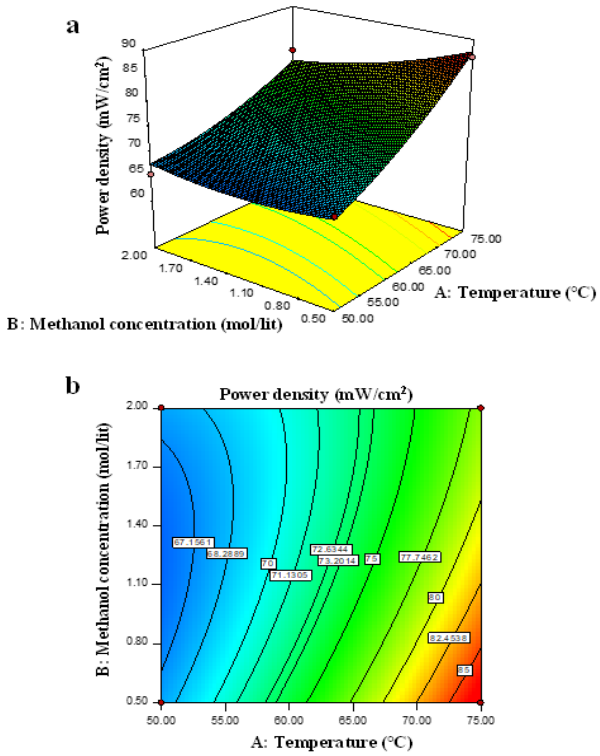

Figure 6. The response surface and contour graphs showing the effects of methanol concentration and temperature on the power density.

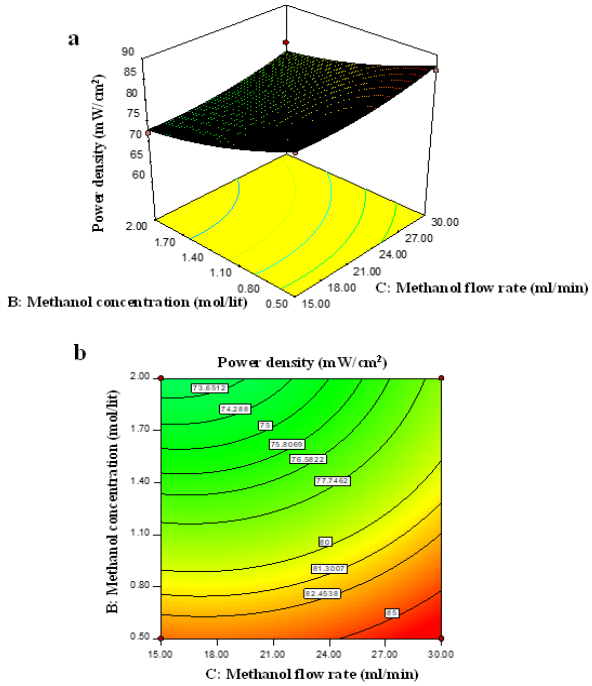

Figure 7. The response surface and contour graphs showing the effects of methanol concentration and methanol flow rate on the power density.

Figure 8 illustrates the stack power density versus temperature and methanol flow rate at a methanol concentration value of 0.5 M and an oxygen flow rate value of 1800 ml min^{-1}. It reveals that increasing the flow rate of methanol leads to an increase in stack power density. The high methanol flow rate can be efficient in the removal of carbon dioxide bubbles on the anode side; however, it leads to more crossover of methanol through the membrane.

The 3D graph and its corresponding contour plot of the model for power density, as affected by the temperature and oxygen flow rate, are given in Figure 9. It can be seen from the response surface plot that increasing the flow rate of oxygen up to a certain point causes an increase in power density. In general, the high oxygen flow rate is required to remove liquid water from the cathode flow channels and enhance oxygen concentration. The excessive oxygen can dry out the backing layer and membrane and decrease the proton conductivity.

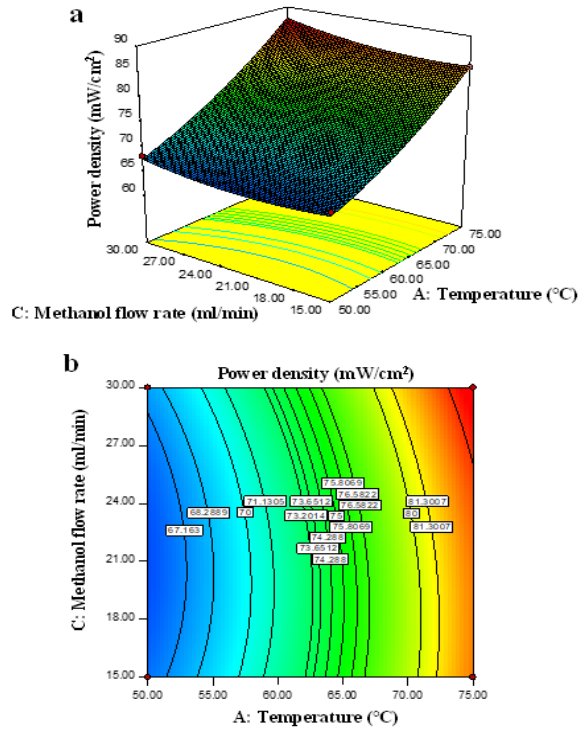

Figure 8. The response surface and contour graphs showing the effects of methanol flow rate and temperature on the power density.

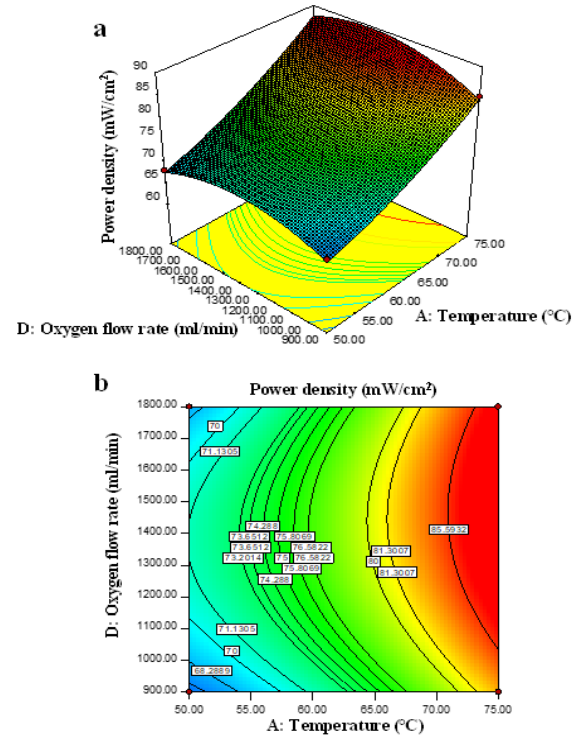

Figure 9. The response surface and contour graphs showing the effects of oxygen flow rate and temperature on the power density.

In this work, an optimization approach was applied to determine the optimum values of operating variables for response from the regression model. The optimum points of the factors and maximum power density are predicted through the regression equation (Eq. (14)). As shown in Table 6, the experimental value of 86.45 mW cm^{-2} for the power density was very close to the predicted value (87.59 mW cm^{-2}). In addition, low error was achieved, confirming that RSM was suitable to optimize the variables of DMFC stack.

Table 6. Validation between the optimized power density obtained from the regression model and the experimental data.

Temperature	Methanol concentration	Methanol flow rate	Oxygen flow rate	Power density
Optimized power density obtained from CCD (predicted value):				
75	0.5	30	1800	87.59
Confirmation study of optimized power density (experimental data):				
75	0.5	30	1800	86.45
				1.32 %

4. CONCLUSIONS

In this study, the maximum power density under the optimum operating conditions (temperature, methanol concentration, methanol flow rate, and oxygen flow rate) of a DMFC stack was obtained using the response surface method. The main findings of this study are summarized below:

- The coefficient of determination (R^2 = 0.9421) was obtained based on the analysis of variance results, showing high prediction accuracy of the second-order model.
- The optimum values of the cell temperature, methanol concentration, methanol, and oxygen flow rates were 75 °C, 0.5 M, 30 ml min^{-1}, and 1800 ml min^{-1}, respectively.
- The power density predicted (87.59 mW cm^{-2}) by the quadratic model had a reasonable error (1.32 %) related to experimental value (86.45 mW cm^{-2}).
- The results showed that the model obtained by RSM was adequate and suitable to be used for optimizing the operating conditions of DMFC stack with minimum cost and time.

5. ACKNOWLEDGEMENT

The authors appreciatively acknowledge the Research Council of the University of Sistan and Baluchestan for their financial support of the project and for providing financial support in setting up Department of Chemical Engineering FC research Lab. Special acknowledge goes to Dokuz Eylul University, Buca, Izmir, Turkey, whose Lab computational resources we have used.

REFERENCES

1. Colpan, C.O., Dincer, I. and Hamdullahpur, F., Portable fuel cells-Fundamentals, technologies and applications, In: Kakac, S., Pramuanjaroenkij, A. and Vasiliev, L., editors, Mini-micro fuel cells: Fundamentals and applications, NATO science for peace and security series, Springer, Netherlands, (2008), 87-101.
2. Wang, C.Y., In: Kakac, S., Pramuanjaroenkij, A. and Vasiliev, L., editors, Mini-micro fuel cells: Fundamentals and applications, NATO science for peace and security series, Springer, Netherlands, (2008), 235-242.
3. Ge, J. and Liu, H., "Experimental studies of a direct methanol fuel cell", ***Journal of Power Sources***, Vol. 142, No. 1-2, (2005), 56-69. (DOI: 10.1016/j.jpowsour.2004.11.022).
4. Argyropoulos, P., Scott, K. and Taama, W.M., "The effect of operating conditions on the dynamic response of the direct methanol fuel cell", ***Electrochimica Acta***, Vol. 45, No. 12, (2000), 1983-1998. (DOI: 10.1016/S0013-4686(99)00420-X).
5. Seo, S.H. and Lee, C.S., "Effect of operating parameters on the direct methanol fuel cell using air or oxygen as an oxidant gas", ***Energy & Fuels***, Vol. 22, No. 2, (2008), 1212-1219. (DOI: 10 .10 21/ef700677y).
6. Jung, D.H., Lee, C.H., Kim, C.S. and Shin, D.R., "Performance of a direct methanol polymer electrolyte fuel cell", ***Journal of Power Sources***, Vol. 71, No. 1-2, (1998), 169-173. (DOI: 10.1016/S0378-7753(97)02793-6).
7. Sharifi, S., Rahimi, R., Mohebbi-Kalhori, D. and Colpan, C.O., "Numerical investigation of methanol crossover through the membrane in a direct methanol fuel cell", ***Iranian Journal of Hydrogen and Fuel Cell***, Vol. 5, No. 1, (2018), 21-33. (DOI: 10.22104/IJHFC.2018.2867. 1170).
8. Myers, R.H. and Montgomery, D.C., Response surface methodology: Process and product optimization using designed experiments, John Wiley and Sons, USA, (2002).
9. Taymaz, I., Akgun, F. and Benli, M., "Application of response surface methodology to optimize and investigate the effects of operating conditions on the performance of DMFC", ***Energy***, Vol. 36, No. 2, (2011), 1155-1160. (DOI: 10.1016/j.energy.2010.11.034).
10. Silva, V.B. and Rouboa, A., "Optimizing the DMFC operating conditions using a response surface method", ***Applied Mathematics and Computation***, Vol. 218, No. 12, (2012), 6733-6743. (DOI: 10.1016/j.amc.2011.12.039).
11. Charoen, K., Prapainainar, C., Sureeyatanapas, P., Suwannaphisit, T., Wongamornpitak, K., Kongkachuichay, P., Holmes, S.M. and Prapainainar, P., "Application of response surface methodology to optimize direct alcohol fuel cell power density for greener energy production", ***Journal of Cleaner Production***, Vol. 142, (2017), 1309-1320. (DOI: 10.1016/j.jclepro.2016.09.059).
12. Yuan, Z., Yang, J., Zhang, Y. and Zhang, X., "The optimization of air-breathing micro direct methanol fuel cell using response surface method", ***Energy***, Vol. 80, No. 1, (2015), 340-349. (DOI: 10.1016/j.energy.2014.11.076).
13. Ordonez, M., Tariq Iqbal, M., Quaicoe, J.E. and Lye, L.M., "Modeling and optimization of direct methanol fuel cells using statistical design of experiment methodology", ***Proceedings of Canadian Conference on Electrical and Computer Engineering***, (2006), 1120–1124. (DOI: 10.1109/CCECE.2006.277802).
14. Liu, Y., Xie, X., Shang, Y., Li, R., Qi, L., Guo, J. and Mathur, V.K., "Power characteristics and fluid transfer in 40 W direct methanol fuel cell stack", ***Journal of Power Sources***, Vol. 164, No. 1, (2007), 322-327. (DOI: 10.1016/j.jpowsour.2002.09.017).
15. Sasmito, A.P., Kurnia, J.C., Shamim, T. and Mujumdar, A.S., "Optimization of an open-cathode polymer electrolyte fuel cells stack utilizing Taguchi method", ***Applied Energy***, Vol. 185, (2017), 1225-1232. (DOI: 10.1016/j.apenergy.2015.12.098).
16. Yu, W., Wu, S. and Shiah, S., "Experimental analysis of dynamic characteristics on the PEM fuel cell stack by using Taguchi approach with neural networks", ***International Journal of Hydrogen Energy***, Vol. 35, No. 20, (2010), 11138-11147. (DOI: 10.1016/j.ijhydene. 2010.07.007).
17. Macedo-Valencia, J., Sierra, J.M., Figueroa-Ramírez, S.J., Díaz, S.E. and Meza, M., "3D CFD modeling of a PEM fuel cell stack", ***International Journal of Hydrogen Energy***, Vol. 41, No. 48, (2016), 23425-23433. (DOI: 10.1016/j. ijhydene.2016.10.065).
18. Liso, V., Simon Araya, S., Olesen, A., Nielsen, M. and Kær, S., "Modeling and experimental validation of water mass balance in a PEM fuel cell stack", ***International Journal of Hydrogen Energy***, Vol. 41, No. 4, (2016), 3079-3092. (DOI: 10.1016/j.ijhydene.2015.10.095).
19. Philipps, S.P. and Ziegler, C., "Computationally efficient modeling of the dynamic behavior of a portable PEM fuel cell stack", ***Journal of Power Sources***, Vol. 180, No. 1, (2008), 309-321. (DOI: 10.1016/j. jpowsour.2008.01.089).
20. Nguyen, G., Sahlin, S., Andreasen, S., Shaffer, B. and Brouwer, J., "Dynamic modeling and experimental investigation of a high temperature PEM fuel cell stack", ***International Journal of Hydrogen Energy***, Vol. 41, No. 8, (2016), 4729-4739. (DOI: 10.1016/j.ijhydene.2016.01.045).
21. Amirfazli, A., Asghari, S. and Koosha, M., "Mathematical modeling and simulation of thermal management in polymer electrolyte

membrane fuel cell stacks", ***Journal of Power Sources***, Vol. 268, (2014), 533-545. (DOI: 10.1016/j.jpowsour.2014.06.073).

22. Shimpalee, S., Ohashi, M., Van Zee, J.W., Ziegler, C., Stoeckmann, C., Sadeler, C. and Hebling, C., "Experimental and numerical studies of portable PEMFC stack", ***Electrochimica Acta***, Vol. 54, No. 10, (2009), 2899-2911. (DOI: 10.1016/j.electacta.2008.11.008).
23. Liu, Z., Mao, Z., Wang, C., Zhuge, W. and Zhang, Y., "Numerical simulation of a mini PEMFC stack", ***Journal of Power Sources***, Vol. 160, No. 2, (2006), 1111-1121. (DOI: 10.1016/j.jpowsour. 2006.03.001).
24. Qin, Y., Liu, G., Chang, Y. and Du, Q., "Modeling and design of PEM fuel cell stack based on a flow network method", ***Applied Thermal Engineering***, Vol. 144, (2018), 411-423. (DOI: 10.1016/ j.applthermaleng.2018.08.050).
25. Drakselová, M., Kodým, R., Šnita, D., Beckmann, F. and Bouzek, K., "Three-dimensional macrohomogeneous mathematical model of an industrial-scale high-temperature PEM fuel cell stack", ***Electrochimica Acta***, Vol. 273, (2018), 432-446. (DOI: 10.1016/j.electacta. 2018.04.042).
26. Argyropoulos, P., Scott, K. and Taama, W.M., "Modeling flow distribution for internally manifolded direct methanol fuel cell stacks", ***Chemical Engineering & Technology***, Vol. 23, (2000), 985-995. (DOI: 10.1002/ 1521-4125(200011)23:11<985::AID-CEAT985>3.0.CO;2-D).
27. Argyropoulos, P., Scott, K. and Taama, W.M., "One-dimensional thermal model for direct methanol fuel cell stacks: Part I. Model development", ***Journal of Power Sources***, Vol. 79, No. 2, (1999), 169-183. (DOI: 10. 1016/S0378-7753(99)00181-0).
28. Simoglou, A., Argyropoulos, P., Martin, E.B., Scott, K., Morris, A.J. and Taama, W.M., "Dynamic modelling of the voltage response of direct methanol fuel cells and stacks: Part I. Model development and validation", ***Chemical Engineering Science***, Vol. 56, No. 23, (2001), 6761-6772. (DOI: 10.1016/S0009-2509 (01)00144-0).
29. Scott, K., Argyropoulos, P. and Taama, W.M., "Modelling transport phenomena and performance of direct methanol fuel cell stacks", ***Chemical Engineering Research and Design***, Vol. 78, No. 6, (2000), 881-888. (DOI: 10.1205/026 387600527941).
30. Kim, D., Lee, J., Lim, T.H., Oh, I.H. and Ha, H.Y., "Operational characteristics of a 50 W DMFC stack", ***Journal of Power Sources***, Vol. 155, No. 2, (2006), 203-212. (DOI: 10.1016/j.jpowsour. 2005.04.033).
31. Lohoff, A.S., Kimiaie, N. and Blum, L., "The application of design of experiments and response surface methodology to the characterization of a direct methanol fuel cell stack", ***International Journal of Hydrogen Energy***, Vol. 41, No. 28, (2016), 12222-12230. (DOI: 10.1016/j.ijhydene.2016.05.248).
32. Santiago, O., Aranda-Rosales, M.A., Navarro, E., Raso, M.A. and Leo, T.J., "Automated design of direct methanol fuel cell stacks: A quick optimization", ***International Journal of Hydrogen Energy***, Vol. 44, No. 21, (2019), 10933-10950. (DOI: 10. 1016/j.ijhydene.2019.02.163).